

Multimetal Rare -Earth MOFs for Lightening and Thermometry: Tailoring Color and Optimal Temperature Range Through Enhanced Disulfobenzoic Triplet Phosphorescence

Richard F. D’Vries,^a Susana Álvarez-García,^a Natalia Snejko,^a Luisa E. Bausá,^b
Enrique Gutiérrez-Puebla,^a Alicia de Andrés^{*a} and M. Ángeles Monge ^{*a}

Supporting Information

Section S1. Experimental details.

Section S2. Fitting profile of experimental and Simulated Powder X-Ray Diffraction Patterns for **RPF-17-Ln**.

Section S3. Thermogravimetric analysis for **RPF-17-Ln**.

Section S4. X-ray powder patterns for **RPF-17-Ln** after TG analysis.

Section S5. Absorption spectra of the 10⁻³ M DSB-Na solution in water

Section S6. Temperature dependence of non-radiative decay

Section S7. Emission spectra of a physical mixture of 50% Eu-DSB and 50% DSB-Na under 270 nm excitation at T= 15 K. The arrows signal the Eu³⁺ absorption lines

Section S8. Powder diffraction patterns for Eu and/or Tb in the multimetal **RPF-17-Gd** samples.

Section S1. Experimental details.

Single-Crystal structure determination. Single-crystal X-ray data for **RPF-17-Gd** was collected in a Bruker-Siemens Smart CCD diffractometer equipped with a normal focus, 2.4 kW sealed tube X-ray source (Mo K α radiation = 0.71073 Å) operating at 50 kV and 30 mA. Data were collected over a hemisphere of the reciprocal space by a combination of three sets of exposure. Each exposure of 20 s covered 0.3° in ω . The unit cell dimension were determined for Least-Square fit of reflections with $I > 20\sigma$. The structures were resolved by direct methods. The final cycles of refinement were carried out by full-matrix least-square analyses with anisotropic thermal parameters of all non-hydrogen atoms. The hydrogen atoms were fixed at their calculated positions using distances and angle constrains. All calculations were performed using SMART software for data collection,¹ SAINT for data reduction² and SHELXTL to resolve and refine the structure.³

X-ray powder diffraction. The characterization by XDR was performed using a Bruker-axs D8 diffractometer (40kV, 30 mA), controlled by a DIFFRACT plus software, in Bragg-Brentano reflection geometry with CuK α radiation ($\lambda = 1.5418\text{Å}$) and PSD detector. The data were obtained between 3 and 30° 2 θ in steps of 0.05° in order to check the purity of the obtained microcrystalline products and to determinate the composition of the residue after TG analysis by comparison of the experimental results with the simulated and reported patterns (ICSD). The data obtained between 3 and 80° 2 θ in steps of 0.05° were used for determinate the isostructurality of the compounds by Le Bail fitting or Profile Matching.⁴ The slit system was selected to ensure that the sample was completely within the X-ray beam at all angles of 2 θ .

Optical measurements. Optical absorption spectra in the 200 – 800 nm range were recorded with a Cary 4000 Varian spectrophotometer. Micro-Raman and Micro-Photoluminescence (PL) spectra were obtained at room temperature with the 488 nm line of and Ar⁺ laser, a microscope (Olympus, BX60M) with a 100x objective, a Super-Notch-Plus Filter (Kaiser Optical Systems) and a N₂ cooled CDD detector coupled to a Jobin-Yvon monochromator.

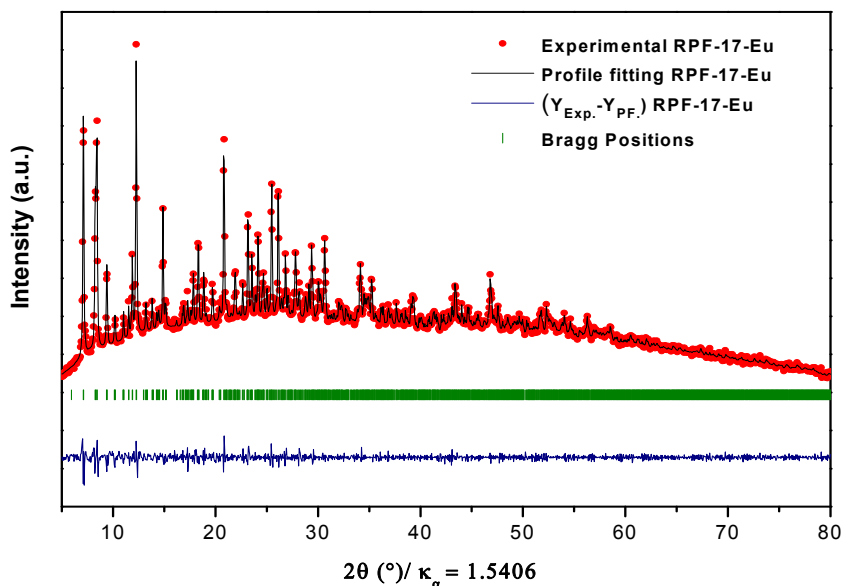
The PL spectra under UV excitation were obtained from pellets. We used the 270 nm line of an OPO laser (NT-342A-SH, EKSPLA) with pulses of 5 ns duration and 10 Hz repetition rate in a quasi-backscattering geometry. The emission was dispersed by a Jobin-Yvon HR 460 monochromator and collected at different delay times after the excitation (usually with a 10 ms gate window) with an intensified CCD digital camera (4Picos, Standford Computer Optics) averaging over 50 laser shots to increase the signal-to-noise ratio. The recorded wavelength range, using a 150 gr/mm diffraction grating, was 200 nm for each image. The PL decay curves were obtained by integrating the images in the spectral range of the particular emission band at increasing delay times after laser pulse. The set up allows obtaining lifetimes from 5 ns, limited by the laser pulse width, to seconds. The measurements at low temperature were recorded with the samples mounted in a continuous flow cryostat from Oxford Instruments. The spectra of the Ln-MOFs were corrected by the instrumental response function. This function was obtained using a tungsten lamp of known spectral emission and a CaF₂ pellet.

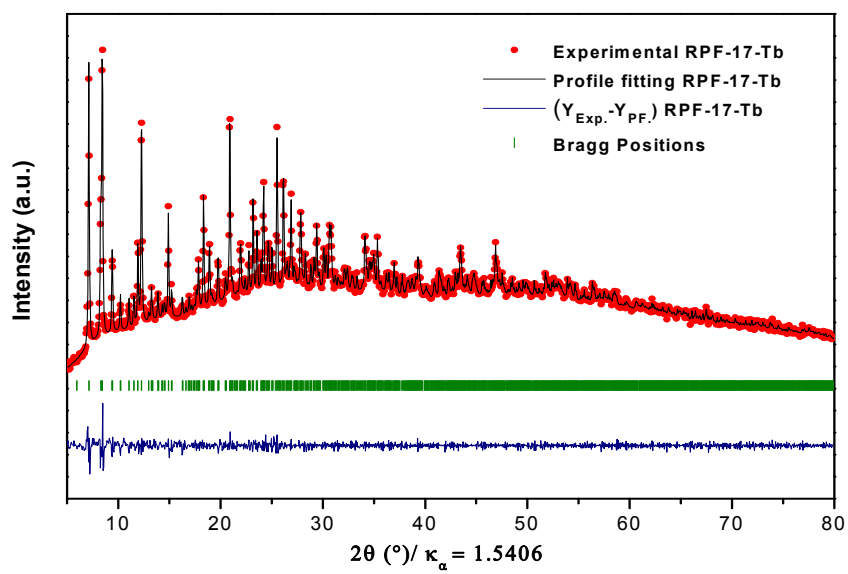
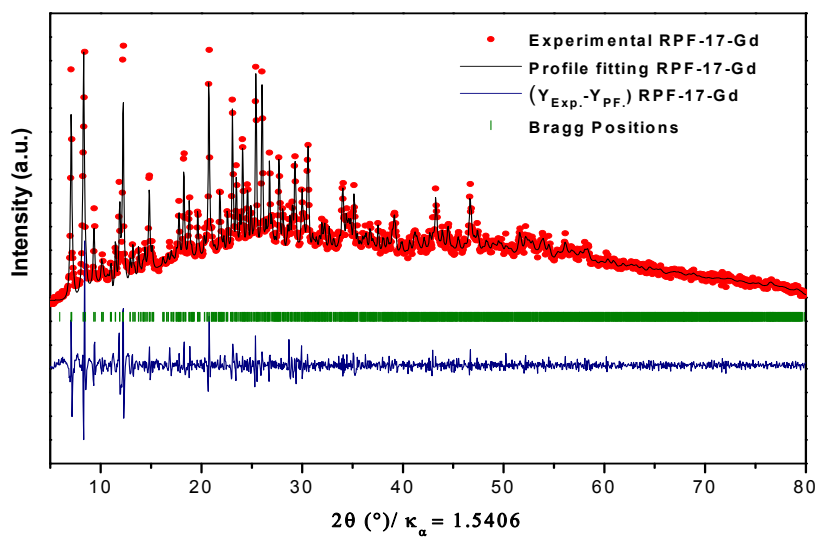
In order to establish a proper comparison among the measured emission intensities we have mixed the same weight of the different compounds under study with a fixed

weight of KBr to obtain identical pellets (5 mm in diameter). In that way, the measurements performed the same day under identical experimental conditions could be reasonably compared. To simplify the notation of the different compounds, in the optical section, we name the $[\text{Ln}_7(3,5\text{-DSB})_4(\text{OH})_9(\text{H}_2\text{O})_{15}] \cdot 4\text{H}_2\text{O}$ compounds as: **Ln-DSB**. When the compound contains several lanthanides the notation indicates their relative proportion at the Ln site.

Section S2. Fitting profile of experimental and Simulated Powder X-Ray Diffraction Patterns for **RPF-17-Ln**.

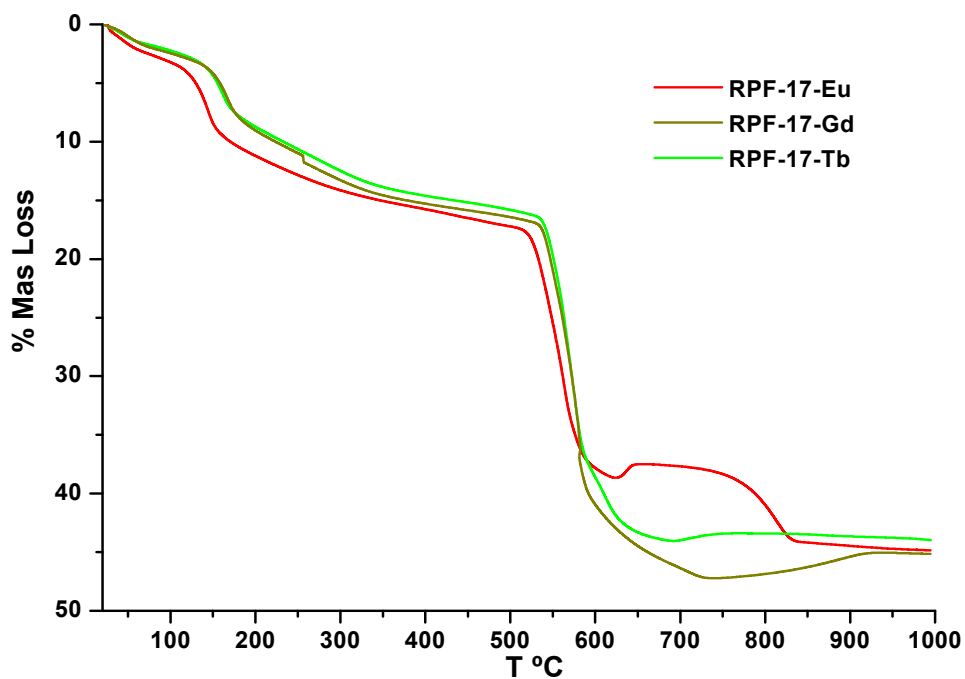
The powder patterns for all the compounds were obtained and compared with the simulated patterns calculated on the basis of the determined crystal structures, using the WinPLOTR^{5, 6} application and the FULLPROF refinement program.⁷ A pseudo-Voigt function was chosen to generate the line shape of the diffraction peaks. The following parameters were refined in the final run: background coefficients, zero-point error, pseudo-Voigt corrected for asymmetry parameters and unit cell parameters. The values for the cell parameters and profile matching refinement are summarized in the Table 2. The results of the refined diffraction pattern profiles show the isostructurality and purity of all these lanthanide materials (**RPF-17-Ln**).



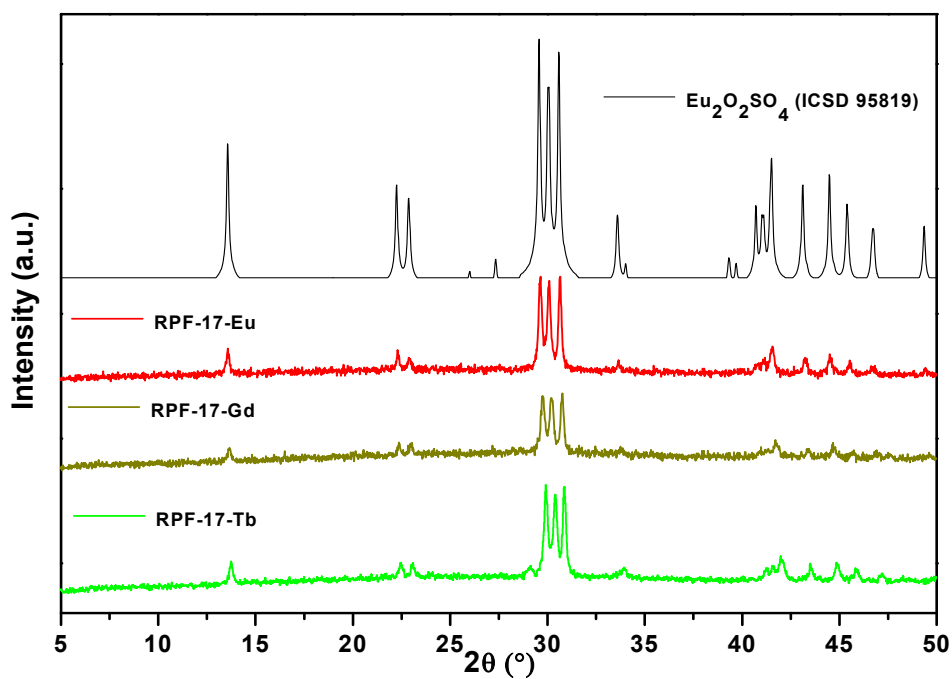


Section S3. Thermogravimetric analysis for **RPF-17-Ln**.

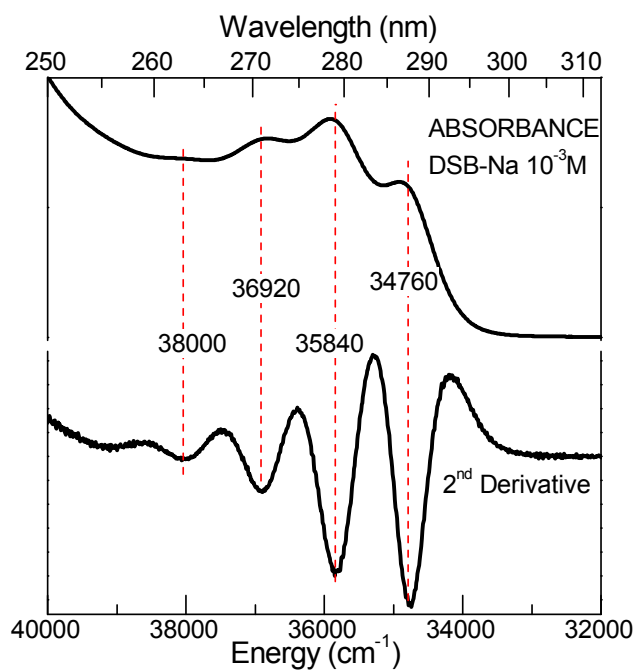
The **RPF-17-Ln** isostructural compounds present similar profile in the decomposition curve with small differences in the temperature of each event. The loss of the crystallization water is observed at low temperature ($\sim 45^\circ\text{C}$) and the coordination water molecules are lost between $100\text{-}150^\circ\text{C}$. Total decomposition of the compounds begins at a temperature between $520\text{-}550^\circ\text{C}$. The decomposition products found for **RPF-17-Ln** compound was $\text{Ln}_2\text{O}_2\text{SO}_4$ (ICSD 95819).⁸ All the decomposition products were confirmed by powder X-ray diffraction comparing the observed patterns with the reported in the ICSD database.



Section S4. X-ray powder patterns for RPF-17-Ln after TG analysis.



Section S5. Absorption spectra of the 10^{-3}M DSB-Na solution in water

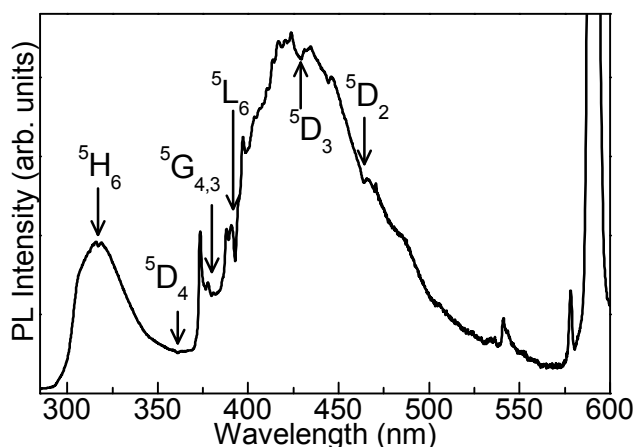


Section S6. According to a phenomenological approximation, the temperature dependence of the probability for non-radiative decay mechanism due to vibrational relaxation is proportional to:

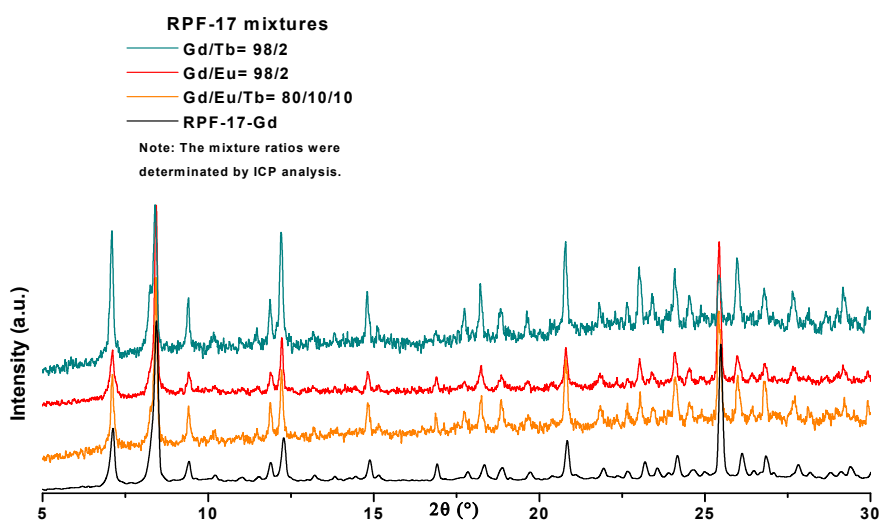
$$(1+n(\Omega,T))^p$$

where p is the number of phonons between the two electronic states: $p = (\Delta E)/h\Omega$, (gap law) and $n(\Omega,T)$ is the population of phonons. Since the measured decay rate is independent of temperature within the measured range, only the highest energy modes may participate in vibration related non-radiative processes. Only OH vibration modes, around 3300 cm^{-1} produce a temperature independent probability.

Section S7. Emission spectra of a physical mixture of 50% Eu-DSB and 50% DSB-Na under 270 nm excitation at $T=15\text{ K}$. The arrows signal the Eu^{3+} absorption lines



Section S8. Powder diffraction patterns for Eu and/or Tb in the MM-RPF-17-Gd samples.



References

1. I. Bruker-Siemens, Madison, WI., 1998.
2. I. Bruker-Siemens, Madison, WI., 1997.
3. I. Bruker-Siemens, Madison, WI., 1998.
4. A. Le Bail, H. Duroy and J. L. Fourquet, *Mater. Res. Bull.*, 1988, **23**, 447-452.
5. T. R. J. Rodriguez-Carvajal., *Materials Science Forum*, 2001, pp. 118-123.
6. J. R.-C. a. T. Roisnel., Commission for Powder Diffraction, International Union of Crystallography. , 1998.
7. R.-C. Juan, *Physica B: Condensed Matter*, 1993, **192**, 55-69.
8. S. G. Zhukov, A. Yatsenko, V. V. Chernyshev, V. Trunov, E. Tserkovnaya, O. Antson, J. Hoelsae, P. Baules and H. Schenk, *Mater. Res. Bull.*, 1997, **32**, 43-50.